

*Supporting information for*

**Insight of Ultrasensitivity and High-stability Flocculation Enhanced Raman Spectroscopy for In-situ Noninvasive Probing of Cupping Effect Substances**

**Meihong Ge,<sup>a,b</sup> Xiuli Zhang,<sup>d</sup> Guoliang Zhou,<sup>a,b</sup> Siyu Chen,<sup>a,b</sup> Zijian Wu,<sup>e</sup> Liaoyuan Li,<sup>e</sup> Yuman Nie,<sup>f</sup> Yaoxiong Wang,<sup>f</sup> Yi Yu,<sup>d</sup> Dongyue Lin,<sup>a,c</sup> Pan Li,<sup>a,c\*</sup> Liangbao Yang,<sup>a,c\*</sup>**

<sup>a</sup>Institute of Health and Medical Technology, Hefei Institutes of Physical Science, Chinese Academy of Sciences, Hefei 230031, China.

<sup>b</sup>University of Science & Technology of China, Anhui, Hefei 230026, China.

<sup>c</sup>Department of Pharmacy, Hefei Cancer Hospital, Chinese Academy of Sciences, Hefei 230031, Anhui, China.

<sup>d</sup>School of Physical Science and Technology, Shanghai Tech University, Shanghai 201210, China.

<sup>e</sup>College of Acupuncture-Moxibustion and Tuina, Anhui University of Chinese Medicine, Hefei 230012, China.

<sup>f</sup>Institute of Intelligent Machines, Hefei Institutes of Physical Science, Chinese Academy of Sciences, Hefei, 230031, China.

**S1. Experimental section. Including figure S1.**

**S2. Analysis and evidence of behaviors of nanoparticles in solution evaporation process. Including figure S2.**

**S3. In situ TEM diagram of flocculation. Including figure S3.**

**S4. Analysis of high speed camera results. Including figure S4, S5, S6.**

**S5. Time-dependent FLERS spectra of 10<sup>-8</sup> M MG. Including figure S7.**

**S6. In situ FLERS spectra after cupping of rats. Including figure S8.**

**S1. EXPERIMENTAL SECTION**

**MATERIALS AND METHODS**

**Materials**

Silver nitrate, sodium citrate, zinc nitrate, hexamethylenetetramine, ammonia water and potassium iodide were bought from Shanghai Chemicals Company. All the chemicals used were of analytical grade or better and were used without further purification. Ultrapure water (>18.0 MΩ·cm) was prepared using a Millipore Milli-Q gradient system throughout the experiment.

### **Silver nanosphere synthesis**

In brief, 1 ml of 0.1 M AgNO<sub>3</sub> was added to 99 ml of Milli-Q water (18.2 MΩ·cm), and heated to 100 °C; 4 ml of 1% sodium citrate was added to the boiling solution under vigorous stirring. The solution was kept boiling for ~1 h. This procedure resulted in a gray-yellow solution. The Ag sols were first washed once; centrifugation of 1000 μL of Ag sols at 8000 r for 10 min was then performed, and 997 μL of the colorless supernatant was discarded. The remaining 3 μL, which contained a black pellet was re-dispersed under sonication. After that, the Ag NPs were used for subsequent experiments.

### **Super hydrophobic silicon wafer treatment**

The super hydrophobic treatment of silicon wafers is achieved by a simple hydrothermal reaction in which a layer of ZnO nanorods is grown on the surface of silicon wafers. The cut 1 cm<sup>2</sup> silicon wafers were placed in a hydrothermal reaction solution (70 ml of 0.015 M zinc nitrate, 70 ml of 0.015 M hexamethylenetetramine and 4 ml of 25% ammonia) and the whole system was placed in a preheated oven at 90 ° C for 24 hours. After the reaction, the silicon wafer was removed, rinsed with deionized water, and dried at room temperature. The silicon is coated with a layer of white zinc oxide.

### **In situ high speed camera measurement**

High speed camera measurements were performed with a FLIR ordinary industrial camera and a MORITEX-RoHS MML1-ST110 lens. After 5 μL of centrifugally concentrated silver sol was added to the surface of the super-hydrophobic silicon wafer, the camera immediately began recording, taking six pictures every minute, until the solvent of the entire sol system was completely evaporated.

### **In situ liquid cell TEM measurement**

We use the small E-chips (Protochips) with a 550 μm × 50 μm window and 150 nm spacer as the bottom chips and the chips with a window size of 550 μm × 50 μm as the top chips. The liquid cell was mounted on the Protochips Poseidon holder, which was inserted into JEOL 2100Plus operated at 200 kV in the experiments.

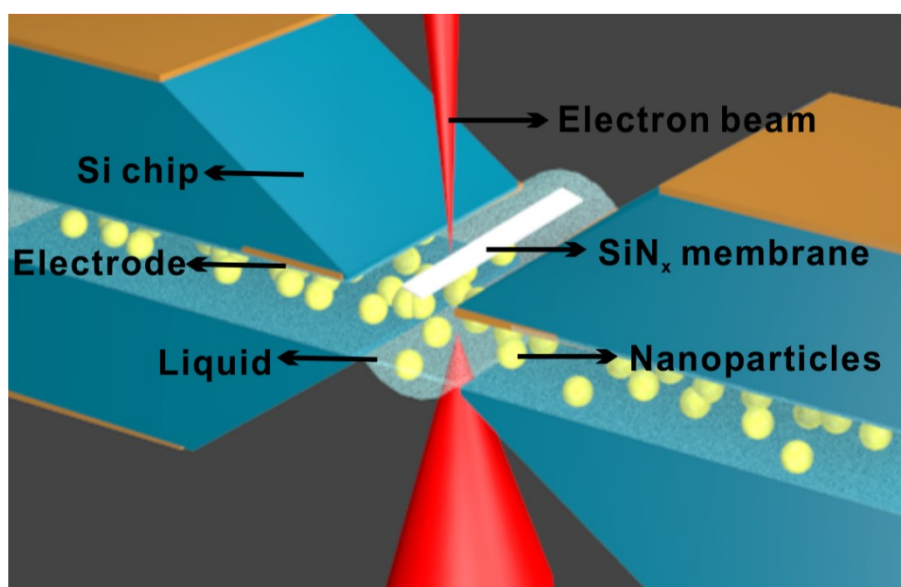


**Figure S1. Schematic diagram of in situ liquid cell TEM detection device.**

Figure S1 is a schematic diagram of the chip used for in situ liquid cell TEM. During the experiment, once we place the sample in the detection chip, the sample is sealed and will remain in the same state as when it was put in for a long time. Such a sealed chip also ensures the feasibility and reliability of observing the state of nanoparticles at different stages, and enables the behavior analysis of nanoparticles during the state transition process.

### **SERS measurements and data processing**

The FLERS spectra of MG molecules were recorded throughout the laser exposure using the 633 nm diode laser at the indicated intensities. The laser was focused on the sample by a 50×/0.75 N.A. objective, leading to a ~1-2 μm spot size.

### **Details of cupping in rats**

Normal grade healthy male SD rats, purchased from Anhui Experimental Animal Center, License number: SCXK (Anhui) 2011-002, body weight (250±20) g. The animals were disposed of in strict accordance with the Guidelines for The Treatment of Animals issued by the Ministry of Science and Technology, PRC in 2006. Before cupping the rats, we performed hair removal on their hind legs. After depilation, the depilation site was washed with water every day, repeated three times a day for three days, to minimize the interference of impurities on the skin surface of the rats, and then the experiment began. In the unique application part of FLERS, we recorded FLERS spectra throughout a portable Raman spectrometer (SEED3000, Ocean hood, China) with a 785 nm laser. 100 mW laser powers with a 1 s accumulation time were used to determine each spectrum. For all SERS spectra, baseline correction was performed using the LabSpec V5.58.25 software. First, a sample was taken before cupping as a control. After that, a portable vacuum cupping device was

used to cupping the hair removal position of rats for 10 minutes. The colloidal droplets of silver nanoparticles were immediately added to the cupping position, and the portable Raman instrument was used for sampling. After that, samples were taken every 10 minutes until the sol was dry.

### Mass spectrometry experiment

In the mass spectrometry experiment, the instrument we used was Proteomex-LTQ mass spectrometer, using conventional ESI source.

### S2. Analysis and evidence of different behaviors of nanoparticles in solution evaporation process.

#### Schematic diagram of experimental process

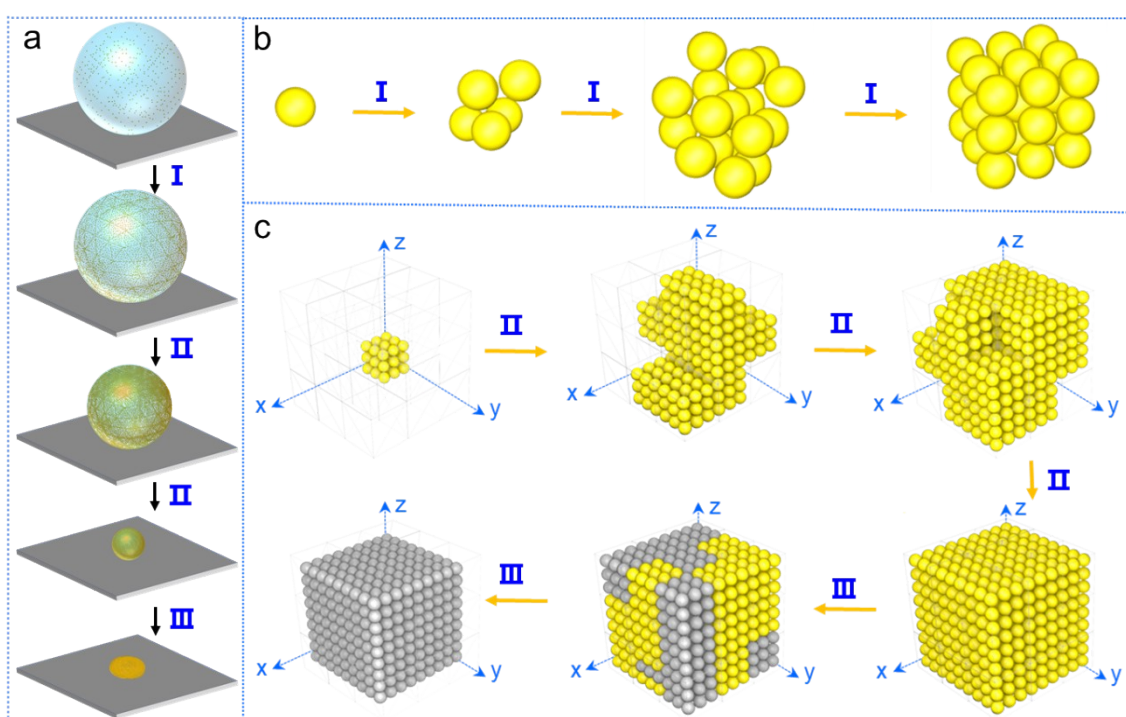


**Figure S2. a. schematic diagram of FLERS detection experiment process. b. corresponding to process I in figure S2.a. nanoparticles form a large number of small flocculation. c. corresponding to process II , III in figure S2.a. small flocculation gradually grow up and further aggregate.**

Figure S2.a shows the FLERS detection experiment process. With the evaporation of the solution, as shown in figure S2.b, numerous small flocculation is first formed in a drop of nanoparticle sol system which correspond to process I in figure S2.a. As the solution further evaporates, the small flocculation gradually grow up (the first four parts of figure S2.c.), and finally the flocculation completely aggregate (the last two parts of figure S2.c).

### S3. In situ liquid cell TEM diagram of flocculation.

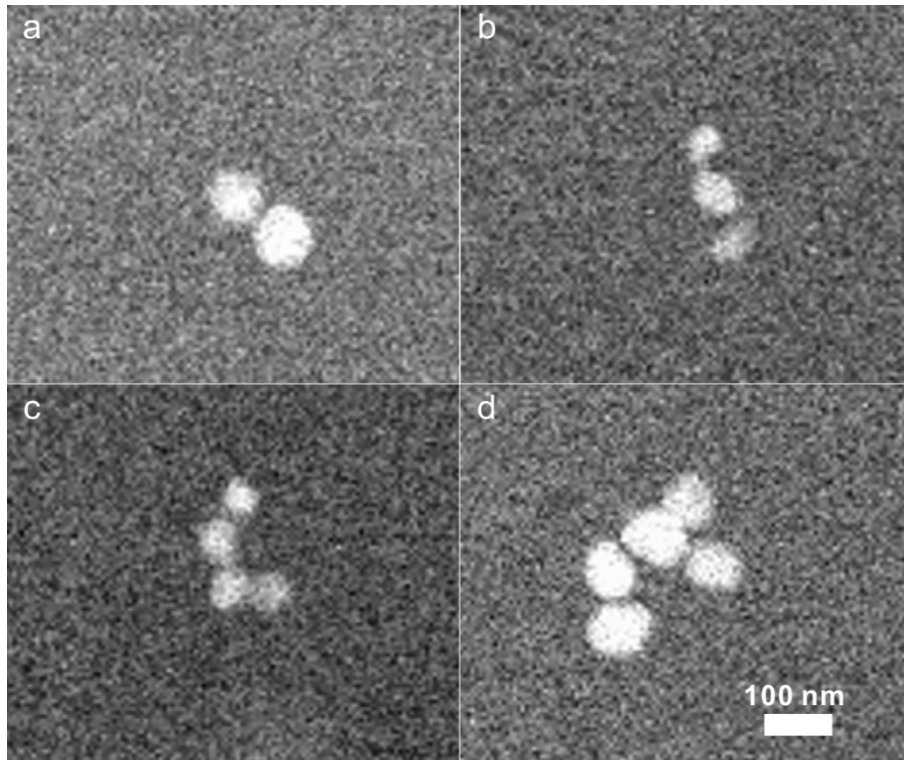


**Figure S3. In situ liquid cell TEM diagram of flocculation in different size.**

By observing the evaporation of silver nanoparticles in different time periods, we always observe flocculation with a certain gap between the nanoparticles. As shown in the figure S3, the gap between the nanoparticles was always 7-9 nm, whether the flocculation made up of two, three or more nanoparticles.

#### **S4. Analysis of high speed camera results.**

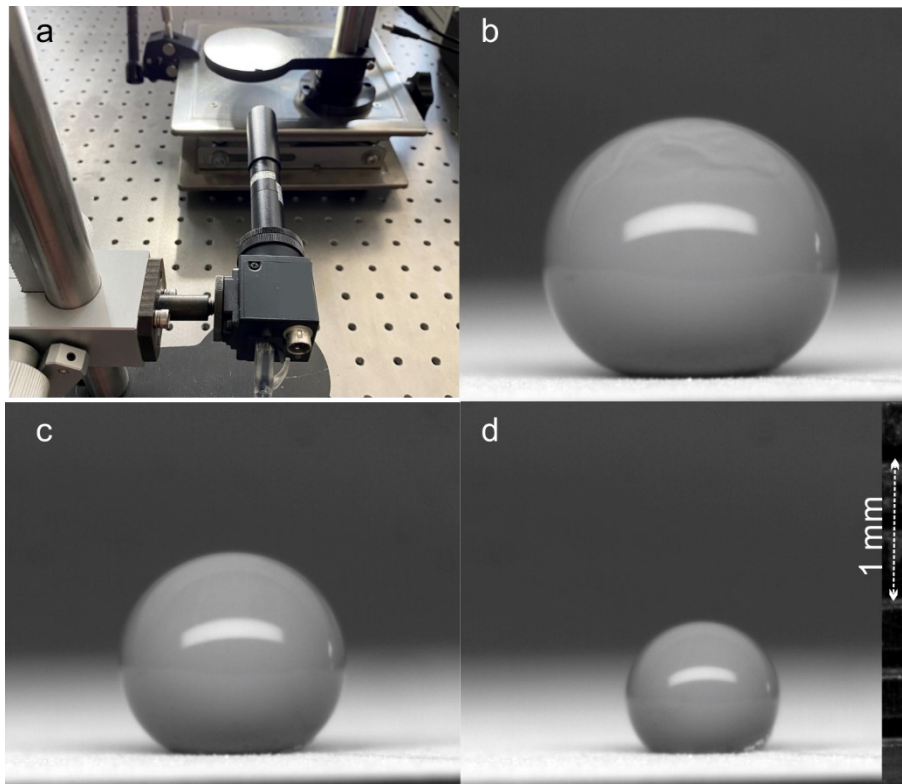


**Figure S4. a, The physical picture of the device set up for the high-speed camera experiment.**

**High speed camera picture of flocculation in different stage during evaporation process (b-d).**

**b.** the initial stage. **c.** the middle stage. **d.** the final stage.

By assembling a FLIR ordinary industrial camera and a MORITEX-RoHS MML1-ST110 lens.

Figure S4.a is the physical picture of the side shooting device. Figure S4.b-d are the high speed camera picture of flocculation in different stage during evaporation process.

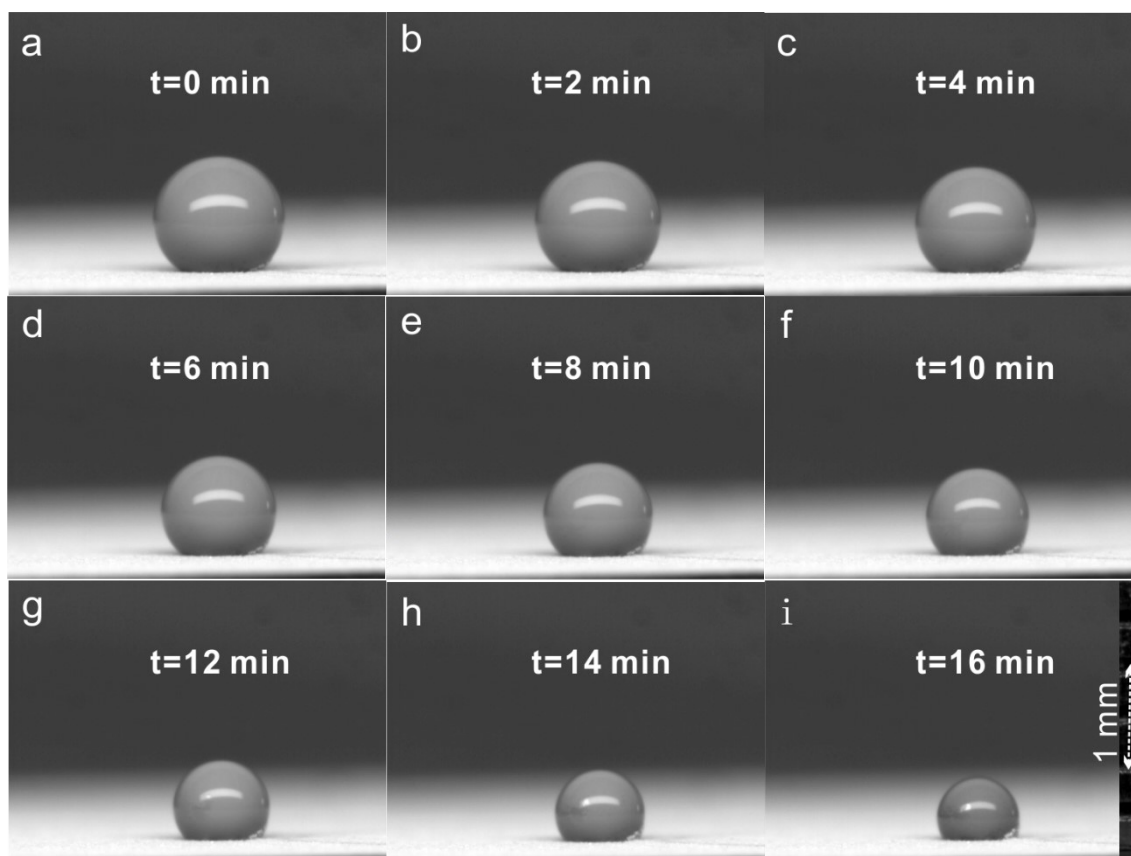


**Figure S5. High speed camera picture of flocculation in different stage during evaporation process.**

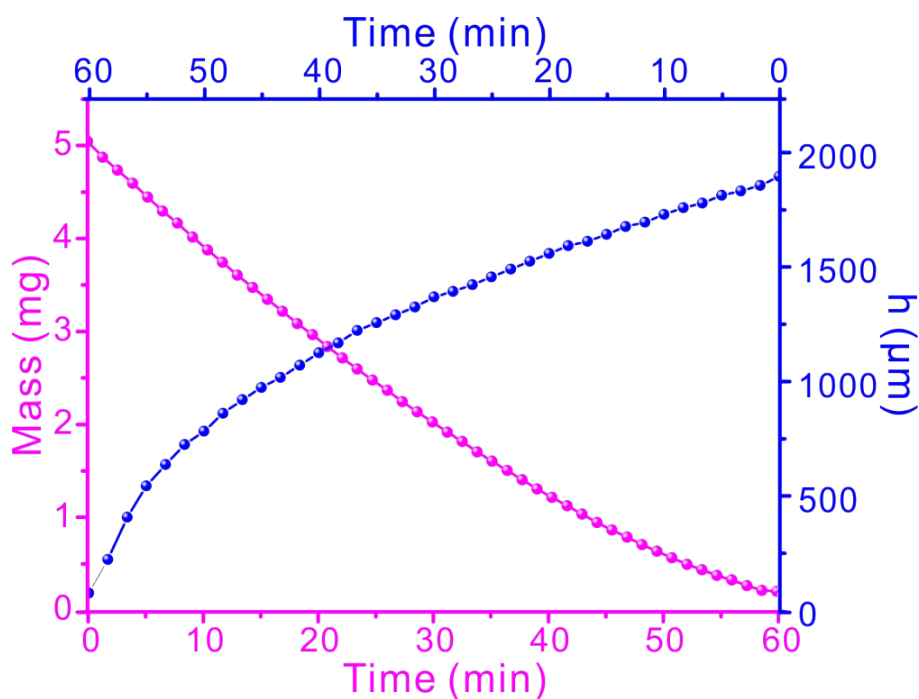


**Figure S6. Spectrum of sol mass and height changing with time during natural evaporation of 5 microliter silver sol.**

Figure S5. a-i records the change of the macroscopic volume of a drop of sol at the flocculation stage. Meanwhile, a balance with an accuracy of  $10 \mu\text{g}$  was used to record the change of sol mass

during this process, as shown in figure S6 (purple line). It can be seen that the height (blue line) and mass of the evaporated sol decrease gradually. Macroscopically, the ionic strength of the whole system gradually increases, and the collision probability of internal flocculation increases. At the same time, the balance between short-range attraction and electrostatic repulsion provides a mechanism to combat instability. Only the flocculation grew up gradually, which did not lead to further agglomeration of nanoparticles in flocculation. So the SERS enhanced effect was improved. The entire process of flocculation growth lasts about 5-10 minutes, enabling efficient and stable detection of FLERS.

#### **S5. Time-dependent FLERS spectra of $10^{-8}$ M MG.**

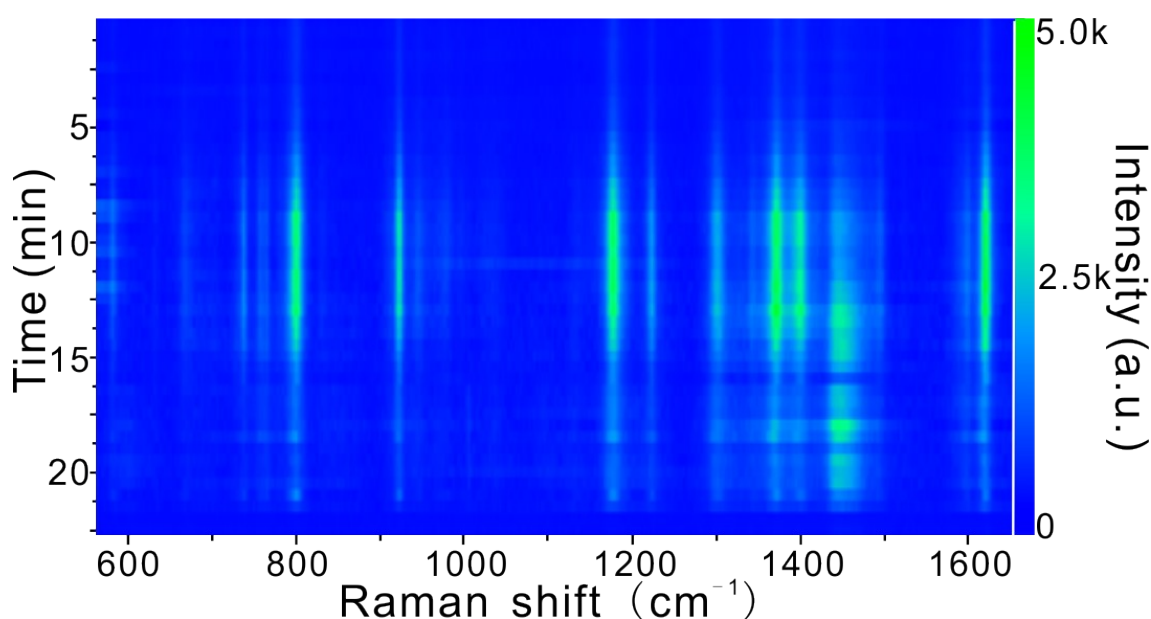


**Figure S7. Time-dependent Raman spectra of  $10^{-8}$  M MG.**

Figure S7 is time-dependent Raman spectra of  $10^{-8}$  M MG. It can be seen from the figure that there is a stable signal phase. This is in good agreement with the results of in situ high-speed photography (figure S5).

#### **S6. In situ monitoring FLERS spectra after cupping of rats.**

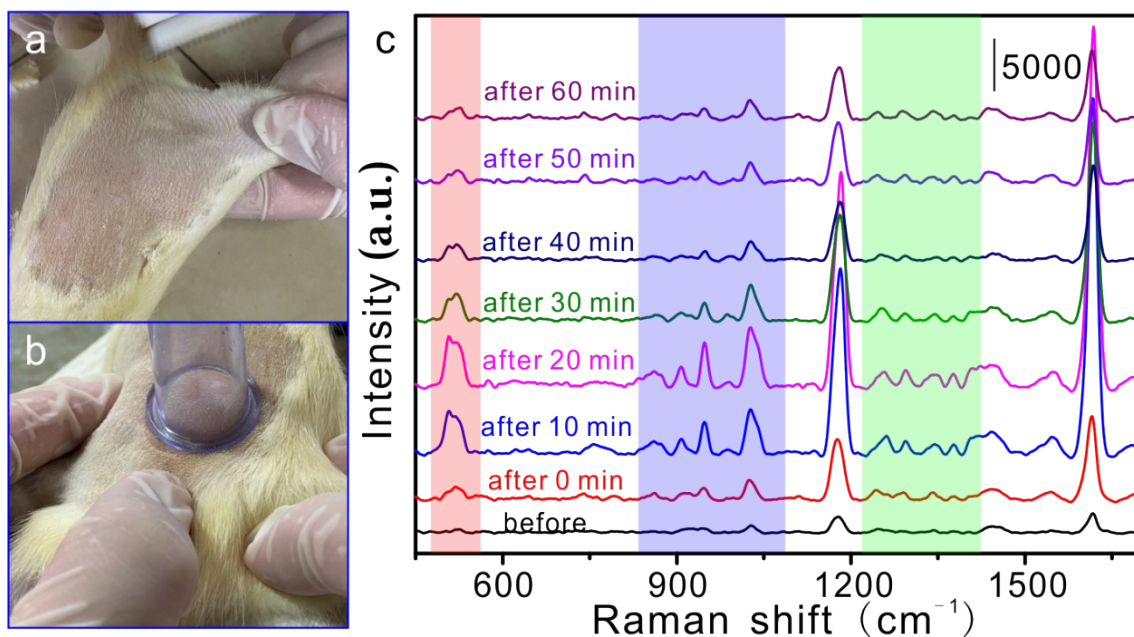


**Figure S8. a. Image of depilation in rats. b. Image of cupping in rats. c. In situ monitoring FLERS spectra after cupping of rats.**

As shown in figure S9.a, after hair removal, cupping was performed on the hind leg of the rat (figure S9.b). FLERS spectra were collected in the cupping area after cupping. Figure S9.c is the FLERS spectrum of in-situ monitoring after cupping. There are three areas (highlighted in red, blue and green in figure S9.c) with significant peak position changes compared to those before cupping (black line in figure S9.c), which are characterized by the generation of new peaks. It can be speculated that some substances are produced on the skin surface of rats after cupping, which is helpful to analyze the internal scientific mechanism of cupping in traditional Chinese medicine.